

Numerical calculation of high frequency magnetic susceptibility in thin nanocrystalline magnetic films



A.V. Izotov^{a,b}, B.A. Belyaev^{a,b}, P.N. Solov'ev^{a,b,*}, N.M. Boev^{a,b}

^a Kirensky Institute of Physics, Federal Research Center KSC SB RAS, 50/38 Akademgorodok, 660036 Krasnoyarsk, Russia

^b Siberian Federal University, 79 Svobodny pr., 660041 Krasnoyarsk, Russia

ARTICLE INFO

Keywords:

Micromagnetic simulation
Magnetization dynamics
Magnetic susceptibility
Ferromagnetic resonance
Nanocrystalline film
Soft magnetic film

ABSTRACT

Two numerical micromagnetic methods most suitable for calculation of the high frequency magnetic susceptibility of nanocrystalline thin films were considered in detail. The methods are based on the Landau–Lifshitz equation, linearized around the equilibrium state leading to an eigenvalue problem or solved using an undetermined coefficients technique. An analysis and estimation of an efficiency of the methods were carried out. Several conclusions about their advantages and shortcomings, as well as specifics of their practical application were drawn.

1. Introduction

Nanocrystalline soft magnetic thin films are nowadays subject to an intense research activity because of great prospects of their practical applications [1,2]. High-frequency magnetic susceptibility studies of nanocrystalline thin films provide relevant information on the strength and dispersion of the anisotropy [3], the anisotropy nature [4], saturation magnetization [5], as well as on the dynamical processes and loss mechanisms [6]; all of them are important for technical applications [7].

The use of numerical methods of micromagnetic theory [8,9] makes it possible to bring out these studies to a qualitatively new level. In particular, with the help of the micromagnetic simulation, in nanocrystalline thin magnetic films it was possible to investigate correlation characteristics of a nonuniform magnetization and to advance our understanding of formation processes of a magnetic microstructure [10–12], to study the magnetization reversal and to establish an influence of structural [12,13] and technological [14,15] parameters on the coercive force and the residual magnetization.

However, the micromagnetic simulation of high-frequency properties of nanocrystalline thin magnetic films [16,17] is not so widely used in practice because of the large computational difficulties encountered in solving such problems. First, because magnetic anisotropy of individual crystallites distributed randomly in the film, the investigation of magnetization dynamics in the non-uniform film is possible only statistically. Consequently, to obtain relevant and reliable results from modelling it is necessary to consider a large (statistically significant)

number of nanocrystallites in a model. Second, fluctuations of an internal magnetic field in nanocrystalline thin magnetic films lead to an almost continuous spectrum of magnetization oscillations excited by a homogeneous alternating magnetic field. Therefore, as a rule, it is impossible to use only individual components of this spectrum in the study of high-frequency properties of nanocrystalline films, as this may result in significant errors.

In this paper we consider in detail two numerical micromagnetic methods which can equally be used to study the magnetization dynamics of uniform and nonuniform ferromagnetic objects of arbitrary shape and volume. However, the main focus of the paper is on the study and analysis of the capabilities of these methods for solving magnetization dynamics problems in nanocrystalline thin films. In Section 2 we first consider a micromagnetic model of a nanocrystalline thin film and carry out the linearization of the Landau–Lifshitz equation. Then in this section we consider two methods for solving a system of linearized Landau–Lifshitz equations: a method based on eigenmodes series expansion of the solution and an undetermined coefficients method. Section 3 presents results of the numerical simulation of the high-frequency magnetic susceptibility of nanocrystalline thin films obtained using these methods. An analysis and estimation of an efficiency of the methods are carried out. Finally, several conclusions about their advantages and shortcomings, as well as specifics of their practical application are drawn.

* Corresponding author. Kirensky Institute of Physics, Federal Research Center KSC SB RAS, 50/38 Akademgorodok, 660036 Krasnoyarsk, Russia.

E-mail address: platon.solov'ev@gmail.com (P.N. Solov'ev).

2. Magnetic susceptibility calculations

2.1. Micromagnetic model

To investigate the properties of nanocrystalline thin magnetic films we will use the following expression for the free energy F given by the micromagnetic theory [8].

$$F = \int_V [-\mathbf{H} \cdot \mathbf{M} + \frac{A}{M_s^2} (\nabla \mathbf{M})^2 - \frac{1}{2} \mathbf{H}^m \cdot \mathbf{M} - \frac{K_u}{M_s^2} (\mathbf{M} \cdot \mathbf{n})^2 - \frac{K}{M_s^2} (\mathbf{M} \cdot \mathbf{l})^2] dV. \quad (1)$$

In this expression, the first term describes the Zeeman energy due to an external magnetic field \mathbf{H} ; the second describes the energy of the exchange interaction with the exchange stiffness constant A ; the third term describes the energy of the demagnetizing field \mathbf{H}^m ; the fourth term describes the energy of the overall for the film uniaxial magnetic anisotropy with a constant K_u and an easy axis unit vector \mathbf{n} . The last term of the expression represents the energy of the uniaxial magnetic anisotropy K with the random orientation of easy axes of magnetization $\mathbf{l} = \mathbf{l}(\mathbf{r})$ in crystallites. The distribution of magnetization is described by the $\mathbf{M}(\mathbf{r})$ vector, which modulus is a constant $|\mathbf{M}(\mathbf{r}, t)| = M_s$.

The demagnetizing field \mathbf{H}^m is determined from the following magnetostatic Maxwell equations: $\text{rot}(\mathbf{H}^m) = 0$ and $\text{div}(\mathbf{H}^m) = -4\pi \text{div}(\mathbf{M})$. In the general case, \mathbf{H}^m can be expressed through a symmetric tensor which describes magnetostatic interaction $G^m \in \mathbb{R}^{3 \times 3}$ [18]

$$\mathbf{H}^m(\mathbf{M}, \mathbf{r}) = \int_V G^m(\mathbf{r} - \mathbf{r}') \mathbf{M}(\mathbf{r}') dV'. \quad (2)$$

In our discrete model we subdivide the continuous thin film into N identical cuboid cells with the volume V_0 and magnetization vectors \mathbf{M}_i ($i = 1, 2, \dots, N$). It is assumed that the magnetization inside each cell is homogeneous. In this case, the expression for the free energy (1) can be written as [13].

$$F = -V_0 \sum_{i=1}^N [\mathbf{H}_i \cdot \mathbf{M}_i + \frac{1}{2} \sum_{j=1}^N \mathbf{M}_i G_{ij} \mathbf{M}_j], \quad (3)$$

where G_{ij} is a 3×3 tensor which describes interactions between i and j discrete elements. The tensor G_{ij} does not depend on the magnetization orientation, it is only determined by intrinsic properties of the investigated magnetic system: $G_{ij} = G_{ij}^e + G_{ij}^m + G_{ij}^u + G_{ij}^a$, where the tensors G_{ij}^e and $G_{ij}^m \in \mathbb{R}^{3 \times 3}$ characterize respectively the exchange and magnetostatic interactions, G_{ij}^u and $G_{ij}^a \in \mathbb{R}^{3 \times 3}$ describe respectively film's overall and random uniaxial magnetic anisotropies. The elements of the symmetric tensors which represent the exchange interaction and uniaxial magnetic anisotropies are given by

$$G_{ij}^e = \frac{2J}{M_s^2} E \text{ (for nearest neighbors } i, j), G_{ij}^u = \frac{2K_{ui}}{M_s^2} \mathbf{n}_i \otimes \mathbf{n}_j \delta_{ij}, G_{ij}^a = \frac{2K_i}{M_s^2} \mathbf{l}_i \otimes \mathbf{l}_j \delta_{ij}, \quad (4)$$

where $J = A/d^2$, d is the distance between neighbor cells, E is an identity matrix of size 3×3 , the sign \otimes means tensor product, and δ_{ij} is the Kronecker delta.

The energy of the demagnetizing field associated with the magnetostatic interaction between i and j discrete elements is represented by a symmetric tensor

$$G_{ij}^m \equiv G^m(\mathbf{r}_i - \mathbf{r}_j) = \begin{bmatrix} G_{ij}^{m(xx)} & G_{ij}^{m(xy)} & G_{ij}^{m(xz)} \\ G_{ij}^{m(xy)} & G_{ij}^{m(yy)} & G_{ij}^{m(yz)} \\ G_{ij}^{m(xz)} & G_{ij}^{m(yz)} & G_{ij}^{m(zz)} \end{bmatrix}. \quad (5)$$

Its components are usually calculated using either exact analytical expressions obtained in Ref. [18], or an approximation where the interaction between a pair of point magnetic dipoles is considered [13]. Because of the long-range nature of the magnetostatic interaction the

matrix $G^m = (G_{ij}^m) \in \mathbb{R}^{3N \times 3N}$ will be dense. In contrast, according to (4), the matrices related to the exchange interaction and magnetic anisotropy will have relatively small number of nonzero elements. However, as matrix elements $G_{ij}^m \equiv G^m(\mathbf{r}_i - \mathbf{r}_j)$ depend only on a difference vector between centers of the cells i and j , the demagnetizing field (2) can be calculated with the knowledge of only a part of the matrix elements G_{ij}^m , using, for example, the convolution theorem [19].

2.2. Linearization of the Landau-Lifshitz equation

The equation of the magnetization dynamics of the i th cell ($i = 1, \dots, N$) is described by the Landau-Lifshitz equation

$$\frac{\partial \mathbf{M}_i}{\partial t} = -\gamma [\mathbf{M}_i \times \mathbf{H}_i^{\text{eff}}] - \gamma \frac{\alpha}{M_s} \mathbf{M}_i \times [\mathbf{M}_i \times \mathbf{H}_i^{\text{eff}}]. \quad (6)$$

Here, the first term represents the magnetization precession around the local effective magnetic field

$$\mathbf{H}_i^{\text{eff}}(\mathbf{M}_1, \dots, \mathbf{M}_N) = -\frac{1}{V_0} \frac{\delta F}{\delta \mathbf{M}_i} = \mathbf{H}_i + \sum_{j=1}^N G_{ij} \mathbf{M}_j, \quad (7)$$

the second term describes the damping in the system, where γ is the gyromagnetic ratio, and α is a damping parameter.

Eq. (6) is nonlinear, therefore the method of successive approximations is usually used to solve it [20]. By considering both the magnetization and effective magnetic field as the sum of static and dynamic parts, the solution of Eq. (6) is sought in the form

$$\begin{aligned} \mathbf{M}_i &= \mathbf{M}_{0i} + \mathbf{m}_i(t) \\ \mathbf{H}_i^{\text{eff}} &= \mathbf{H}_{0i}^{\text{eff}} + \mathbf{h}_i^{\text{eff}}(t), \end{aligned} \quad (8)$$

where \mathbf{M}_{0i} is the equilibrium magnetization of i th cell, which, as shown in Ref. [13], can be found from the system of linear inhomogeneous equations with undetermined Lagrange multipliers ν_i :

$$\mathbf{H}_{0i}^{\text{eff}}(\mathbf{M}_{01}, \mathbf{M}_{02}, \dots, \mathbf{M}_{0N}) - \nu_i \mathbf{M}_{0i} = 0. \quad (9)$$

According to Eqs. (7) and (9), the static and dynamic parts of the effective field is given by

$$\begin{aligned} \mathbf{H}_{0i}^{\text{eff}} &= \sum_{j=1}^N G_{ij} \mathbf{M}_{0j} + \mathbf{H}_0 = \nu_i \mathbf{M}_{0i} \\ \mathbf{h}_i^{\text{eff}}(t) &= \sum_{j=1}^N G_{ij} \mathbf{m}_j(t) + \mathbf{h}_i^{\text{eff}}. \end{aligned} \quad (10)$$

Under the assumption of small oscillations $|\mathbf{m}_i(t)| \ll |\mathbf{M}_{0i}|$, $|\mathbf{h}_i^{\text{eff}}(t)| \ll |\mathbf{H}_{0i}^{\text{eff}}|$, taking into account the following notation

$$\Lambda(\mathbf{M}_{0i}) \equiv \begin{pmatrix} 0 & -M_{0i}^{(z)} & M_{0i}^{(y)} \\ M_{0i}^{(z)} & 0 & -M_{0i}^{(x)} \\ -M_{0i}^{(y)} & M_{0i}^{(x)} & 0 \end{pmatrix}, \quad \begin{aligned} N_i &= -\gamma(\Lambda(\mathbf{M}_{0i}) + \frac{\alpha}{M_s} (\Lambda(\mathbf{M}_{0i}))^2) \\ B_{ij} &= N_i(G_{ij} - \nu_i \delta_{ij} E) \end{aligned}, \quad (11)$$

linearizing of Eq. (6) leads to the following linear system:

$$\frac{\partial \mathbf{m}_i}{\partial t} = \sum_{j=1}^N B_{ij} \mathbf{m}_j + N_i \mathbf{h}_i^{\text{eff}} \quad (i = 1, \dots, N). \quad (12)$$

The resulting system of equations underlies some of the methods for calculating the dynamic properties of ferromagnets. In this paper, we consider two of them: the solution of Eq. (12) by (i) the eigenvalue-based approach, and by (ii) undetermined coefficients method.

2.3. Solution of the linearized Landau-Lifshitz equation by eigenvalue-based approach

The well-known method to solve system (12) is associated with finding the eigenvectors \mathbf{V}_m and eigenvalues λ_m of the matrix $B = (B_{ij}) \in \mathbb{R}^{3N \times 3N}$ [21–25]. According to this approach, the general solution of system (12) can be written as an expansion in terms of the linearly independent eigenvectors of normal magnetic oscillation

modes

$$\mathbf{m}_j(t) = \sum_{m=1}^M c_m(t) \mathbf{V}_{mj} (j = 1, 2, \dots, N), \quad (13)$$

where $\mathbf{V}_m = [\mathbf{V}_{m1}; \mathbf{V}_{m2}; \dots; \mathbf{V}_{mN}]$, and $\mathbf{V}_{m1}; \mathbf{V}_{m2}; \dots; \mathbf{V}_{mN}$ are the amplitudes of magnetization oscillations in each cell at a frequency of the m th mode, M is the number of oscillation modes taken into account in the calculation ($M \leq 2N$). If the magnetic system is excited by the homogeneous alternating magnetic field $\mathbf{h}^f(t) = \mathbf{h}_0 e^{-i\omega t}$ with a frequency ω , in the steady-state regime $c_m(t)$ is given by Ref. [25].

$$c(t) = \frac{\sum_{i=1}^N \mathbf{U}_{mi} N_i \mathbf{h}_0}{-(\lambda_m + i\omega)} e^{-i\omega t} = -i \frac{(\mathbf{w}_m \cdot \mathbf{h}_0)}{\omega_m - \omega + i\Delta\omega_m} e^{-i\omega t}. \quad (14)$$

Vectors $\mathbf{U}_m = [\mathbf{U}_{m1}; \mathbf{U}_{m2}; \dots; \mathbf{U}_{mN}]$ in Eq. (14) are determined from condition $U = (\mathbf{V}^T \cdot \mathbf{V})^{-1} \mathbf{V}^T$ (here, ‘T’ denotes the transposition, and ‘-1’ indicates the inverse matrix), where $U = (U_m) \in \mathbb{C}^{M \times 3N}$, and $V = (V_{mj}) \in \mathbb{C}^{M \times 3N}$.

The complex eigenvalue of the m th mode is related to the resonance frequency ω_m and the damping $\Delta\omega_m$ of the mode by the expression $\lambda_m = \Delta\omega_m - i\omega_m$. The m th mode will be excited when the so-called ‘excitation integral’ in the numerator of Eq. (14) has a nonzero value. When the external field \mathbf{h}_0 is homogeneous, the ‘excitation integral’ can be expressed as a dot product of vectors \mathbf{h}_0 and $\mathbf{w}_m = \sum_{i=1}^N \mathbf{U}_{mi} N_i$. In this case, the modulus of vector \mathbf{w}_m $A_m = |\mathbf{w}_m|$ characterizes the amplitude of a uniform excitation of the m th mode.

The averaging of $\mathbf{m}_j(t)$ over the volume V leads to

$$\begin{aligned} \mathbf{m}(t) &= \frac{1}{N} \sum_{j=1}^N \mathbf{m}_j = -i \sum_{m=1}^M \frac{\mathbf{v}_m \otimes \mathbf{w}_m}{\omega_m - \omega + i\Delta\omega_m} \mathbf{h}_0 e^{-i\omega t}, \text{ where } \mathbf{v}_m \\ &= \frac{1}{N} \sum_{j=1}^N \mathbf{V}_{mj}. \end{aligned} \quad (15)$$

It is then straightforward to write an expression for the high frequency susceptibility tensor

$$\overleftrightarrow{\chi} = -i \sum_{m=1}^M \frac{\mathbf{v}_m \otimes \mathbf{w}_m}{\omega_m - \omega + i\Delta\omega_m}. \quad (16)$$

2.4. Solution of the linearized Landau–Lifshitz equation by undetermined coefficients method

In another, more simple method [26–29], by substituting $\mathbf{m}_i(t) = \mathbf{m}_{0i} e^{-i\omega t}$ and $\mathbf{h}_i^f(t) = \mathbf{h}_{0i} e^{-i\omega t}$ the system of differential Eq. (12) is reduced to the system of linear inhomogeneous equations

$$-i\omega \mathbf{m}_{0i} = \sum_{j=1}^N B_{ij} \mathbf{m}_{0j} + N_i \mathbf{h}_{0i}. \quad (17)$$

Thereafter system (17) can be solved by using standard numerical methods of linear algebra, for example, conjugate gradient or minimal residual methods. It is important to note that, because of the limitation $|\mathbf{M}_i| = M_s$, only $2N$ of all $3N$ equations of system (17) are linearly independent. This makes it possible to reduce the number of unknowns from $3N$ to $2N$. One way to do this is to transform all magnetic moments to local coordinates, in which the z -axis coincides with the equilibrium direction of the magnetic moment \mathbf{M}_{0i} at this point: $\mathbf{m}'_{0i} = T_i \mathbf{m}_{0i}$; $\mathbf{h}'_{0i} = T_i \mathbf{h}_{0i}$. For this case the transformation matrix T_i can be written as

$$T_i = \begin{bmatrix} \cos \theta_i \cos \phi_i & \cos \theta_i \sin \phi_i & -\sin \theta_i \\ -\sin \phi_i & \cos \phi_i & 0 \\ \sin \theta_i \cos \phi_i & \sin \theta_i \sin \phi_i & \cos \theta_i \end{bmatrix}, \quad (18)$$

where ϕ_i and θ_i are the azimuthal and polar angles of the vector \mathbf{M}_{0i} . In the new coordinate system, the problem become two dimensional, that is, only x and y components of vectors and tensors are considered.

Therefore, we have

$$N' = N'_i = T_i N_i T_i^T = \gamma M_s \begin{bmatrix} \alpha & 1 \\ -1 & \alpha \end{bmatrix}, L' = (N')^{-1} = \frac{1}{\gamma M_s (1 + \alpha^2)} \begin{bmatrix} \alpha & -1 \\ 1 & \alpha \end{bmatrix}. \quad (19)$$

And system (17) then can be written as

$$\sum_{j=1}^N A'_{ij} \mathbf{m}'_{0j} = -\mathbf{h}'_{0i}, \quad (20)$$

where $A'_{ij} = G'_{ij} - v_i \delta_{ij} E + i\omega \delta_{ij} L'$.

It is convenient to rewrite system (20) in the compact matrix form as $Ax = b$, where $A = (A'_{ij}) \in \mathbb{C}^{2N \times 2N}$, $x = (\mathbf{m}'_{0j}) \in \mathbb{C}^{2N \times 1}$, $b = (-\mathbf{h}'_{0i}) \in \mathbb{C}^{2N \times 1}$. The solution of this system and the subsequent transformation to the coordinate system related to the investigated film by $\mathbf{m}_{0i} = T_i^T \mathbf{m}'_{0i}$ gives the solution of the original system of Eq. (17).

For a given pumping field \mathbf{h}_{0k} and a given angular frequency ω , the method enables us to calculate the dynamic magnetization $\mathbf{m}_{0i}(\omega)$. By considering an orthogonal basis of excitation vectors ($\mathbf{h}_{0i}^{(1)}, \mathbf{h}_{0i}^{(2)}, \mathbf{h}_{0i}^{(3)}$) and the resulting response of the magnetic system ($\mathbf{m}_{0i}^{(1)}, \mathbf{m}_{0i}^{(2)}, \mathbf{m}_{0i}^{(3)}$), the local dynamic susceptibility tensor will be given by Ref. [30].

$$\chi_i^{(\alpha\beta)} = \frac{\mathbf{m}_{0i}^{(\alpha)} \cdot \mathbf{h}_{0i}^{(\beta)}}{|\mathbf{h}_{0i}^{(\alpha)}| |\mathbf{h}_{0i}^{(\beta)}|}, (\alpha, \beta = 1, 2, 3) \quad (21)$$

and the high frequency susceptibility tensor averaged over the film's volume will be

$$\chi^{(\alpha\beta)} = \frac{1}{N} \sum_{i=1}^N \chi_i^{(\alpha\beta)}. (\alpha, \beta = 1, 2, 3) \quad (22)$$

It should be noted that methods considered in this paper enable study of magnetization dynamics not only in nanocrystalline thin magnetic films but also in any ferromagnetic objects of arbitrary shape, including multilayer thin-film structures.

3. Numerical simulations

3.1. Modelling details

We have implemented the methods described in the previous section to calculate the high frequency magnetic susceptibility of nanocrystalline thin films. For brevity, we will refer to the eigenvalue-based approach hereinafter as Method 1 and mark it on figures as ‘M1’ while the method of undetermined coefficients for solving of the system of linearized Landau–Lifshitz equations will be denoted as Method 2 or ‘M2’.

The investigated films were monolayers of close-packed nanoparticles with the random distribution of the uniaxial anisotropy axes. The number of particles N were $128 \times 128 \times 1$ and $1024 \times 1024 \times 1$. The size of nanoparticles D coincided with the size of discrete cells and varied from 12 to 100 nm. We used two-dimensional periodic boundary conditions for the exchange and magnetostatic interactions to eliminate the edge effects originating from an inhomogeneity of an internal magnetic field in samples of finite size [31]. For definiteness we chose the film's magnetic parameters corresponding to the well-known nanocrystalline alloy $\text{Fe}_{73.5}\text{Cu}_1\text{Nb}_3\text{Si}_{13.5}\text{B}_9$ [32]: the saturation magnetization $M_s = 955$ emu/cm³ (955 kA/m), the exchange constant $A = 1 \times 10^{-6}$ erg/cm (1×10^{-11} J/m), and the local uniaxial anisotropy field $H_a = 2K/M_s = 171.7$ Oe ($K = 8200$ J/m³). In all calculations, we used the same random distribution of the anisotropy axes. The overall for the entire film uniaxial magnetic anisotropy K_u was not taken into account to ease an analysis of simulation results. The external in-plane magnetic field $\mathbf{H} = 94.744$ Oe (7.54 kA/m) was applied along the x -axis while the in-plane alternating homogeneous field \mathbf{h}_0 was applied along y -axis. The damping parameter $\alpha = 0.005$.

In this study, we only consider the frequency dependence of the

averaged scalar dynamic susceptibility χ along applied alternating field. For both Methods 1 and 2, we used the following formula to calculate χ

$$\chi = \frac{1}{N} \sum_{i=1}^N \frac{\mathbf{m}_{0i} \cdot \mathbf{h}_{0i}}{|\mathbf{h}_{0i}|^2}. \quad (23)$$

To understand the limitations which are met during modelling process let us estimate the computational effort of each method. In Method 1, for computing M eigenvectors of size $2N \times 1$ it is required $O(M \times 2N)$ operations and bytes of RAM. The computation of all magnetic oscillation modes leads to the estimate of $O(4N^2)$. In Method 2, it is required to calculate only $2N$ unknown amplitudes of the dynamic magnetization which results in the estimate of $O(2N)$ for the computational cost. For this reason, when modelling dynamical processes in nanocrystalline magnetic films with the help of Method 1 we used only $128 \times 128 \times 1$ discrete elements. On the other hand, the use of Method 2 allowed us to model films with the number of elements $128 \times 128 \times 1$ and $1024 \times 1024 \times 1$.

3.2. Numerical results and discussion

According to the phenomenological theory of homogeneous ferromagnetic resonance in an isotropic uniformly magnetized thin magnetic film, the imaginary part of the magnetic susceptibility $\chi_u = \chi'_u - i\chi''_u$ can be expressed as [20].

$$\chi''_u(\omega) = \frac{1}{4\pi} \frac{\alpha\omega\omega_M[(\omega_M + \omega_H)^2 + \omega^2]}{(\omega_0^2 - \omega^2)^2 + \alpha^2\omega^2(\omega_M + 2\omega_H)^2}, \quad (24)$$

where $\omega_M = \gamma 4\pi M_s$, $\omega_H = \gamma H$, and the resonance frequency $\omega_0 = 2\pi f_0 = \sqrt{\omega_H(\omega_M + \omega_H)}$. For our parameters $M_s = 955 \text{ emu/cm}^3$ and $H = 94.744 \text{ Oe}$ the resonance frequency f_0 is equal to 3 GHz. The maximum value of χ''_u observed on the resonance frequency is $\chi''_{u0} = \chi''_u(\omega_0) \approx \sqrt{M_s/\pi H}/2\alpha \approx 179$.

In nanocrystalline thin films the random magnetic anisotropy can substantially affect the behavior of $\chi(\omega)$. This is confirmed by the simulation results demonstrated in Figs. 1–3. In particular, insets of Fig. 1 show reduced to χ''_{u0} dependences (24) (solid lines) and dependences χ''/χ''_{u0} calculated by using Method 1 for various sizes of crystallites D (circle markers). All modes of magnetization oscillation were taken into account in the simulation ($M = 2N$), where the number of cells was $N = 128 \times 128 \times 1$.

To analyze the obtained results, we additionally calculated the ratio between the exchange energy $F^e = -VJ = -VA/D^2$ and the energy of the random uniaxial magnetic anisotropy $F^a = -VK = -VM_s H_a/2$ (see Table 1). It is evident from the figures that in films with the ratio $F^e/F^a > 1$ the exchange interaction between crystallites considerably subdues the influence of the local anisotropy. It is especially noticeable for the film with $D = 12 \text{ nm}$, whose exchange energy is more than eight times larger than the energy of the random uniaxial magnetic anisotropy. Its magnetic characteristics are close to that of an isotropic uniformly magnetized film; its dependence of the magnetic susceptibility on frequency is almost identical to the curve obtained using expression (24).

With the increase of the crystallites size the random uniaxial anisotropy energy begins to dominate over the energy of the exchange interaction. This results in a significant broadening and asymmetry of the $\chi''(f)$ line, as well as in a shift of the resonance frequency. If the size of crystallite is larger than the exchange correlation length – which is true for the film with $D = 100 \text{ nm}$, whose random anisotropy energy is more than eight times larger than the exchange energy – then the amplitude of spatial fluctuations of magnetization considerably increases. This results in the maximal transformation of $\chi''(f)$ behavior.

Method 1 has an important advantage over Method 2 since it allows one to calculate the high frequency magnetic susceptibility of nanocrystalline films as well as the structure of the spectrum of resonant

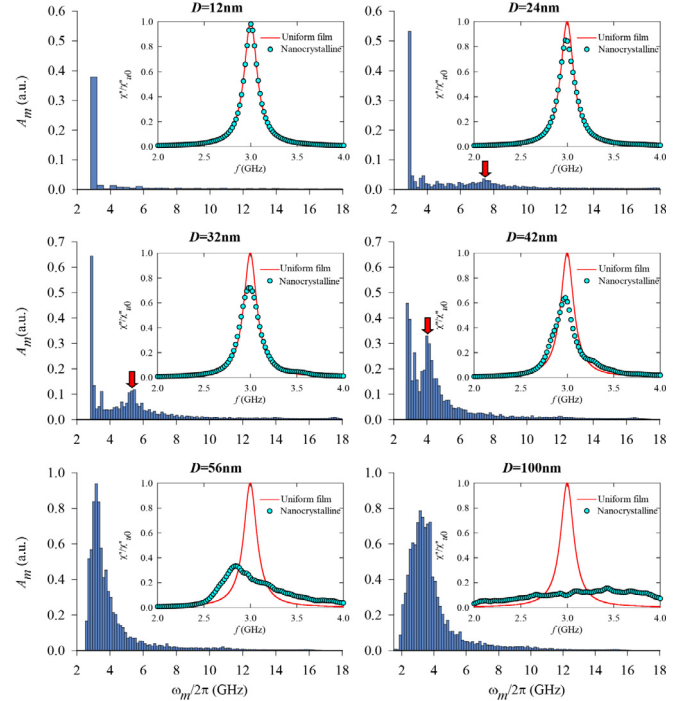


Fig. 1. The frequency distribution of amplitudes A_m of the uniform excitation of normal magnetic oscillation modes for nanocrystalline films with crystallite size $D = 12, 24, 32, 42, 56$ and 100 nm . Insets show the frequency dependence of the imaginary part of the reduced magnetic susceptibility for a uniform (line) and nanocrystalline (circle markers) thin films.

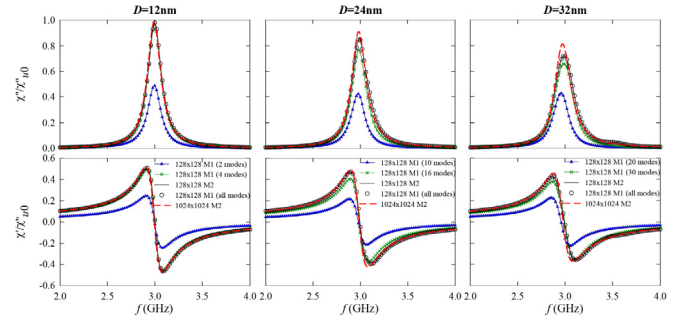


Fig. 2. Frequency dependences of the imaginary (above) and real (below) parts of the reduced high-frequency magnetic susceptibility of nanocrystalline films with crystallite size $D = 12, 24$ and 32 nm .

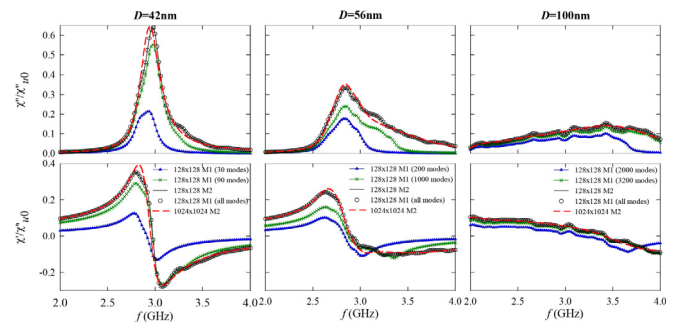


Fig. 3. Frequency dependences of the imaginary (above) and real (below) parts of the reduced high-frequency magnetic susceptibility of nanocrystalline films with crystallite size $D = 42, 56$ and 100 nm .

Table 1

The ratio between the exchange energy F^e and the energy of the random uniaxial magnetic anisotropy F^a of nanocrystalline thin magnetic films for different sizes of crystallites D .

D	12 nm	24 nm	32 nm	42 nm	56 nm	100 nm
F^e/F^a	8.47	2.12	1.19	0.69	0.39	0.12
F^a/F^e	0.12	0.47	0.84	1.45	2.57	8.2

modes excited by an external alternating magnetic field. As an example, Fig. 1 shows the frequency distribution of amplitudes A_m of the uniform excitation of normal magnetic oscillation modes for various crystallite sizes. The increase of the crystallites size leads to a sharp increase in a number of excited modes and a sharp rise in their amplitudes. For the film with $D = 12$ nm merely four first lowest modes form the dynamic susceptibility spectrum almost completely. On the contrary, for the film with $D = 100$ nm practically all modes contribute to the resulting spectrum. It is important to note the additional peak which was revealed in the $A_m(\omega_m)$ distribution for the film with $D = 24, 32$ and 42 nm (marked in figures by an arrow). The nature of this peak and its influence on the magnetic susceptibility will be considered in our subsequent paper.

To compare, analyze and verify methods considered in this paper the real and imaginary parts of the magnetic susceptibility were calculated for different sizes D (see Figs. 2 and 3). The reduced dependences $\chi''(f)/\chi''_{u0}$ and $\chi'(f)/\chi'_{u0}$ calculated using Method 1 are shown in the figures by circle markers. These results were obtained for the numerical model of the film with the number of crystallites equal to $128 \times 128 \times 1$, all $M = 2N = 32768$ modes were taken into account. The same dependences obtained with the help of Method 2 are shown as solid black lines. It is evident that the both methods give the identical results.

However, the time taken to calculate the magnetic susceptibility using Method 1 was more than ten times greater than for Method 2. The common approach for reducing the computational cost (as noted earlier, $O(M \times 2N)$ for Method 1) is to decrease the number of modes M used in the calculation. To study the effect of decreasing the number of modes on the accuracy of obtained results we additionally calculated the dependences $\chi''(f)/\chi''_{u0}$ and $\chi'(f)/\chi'_{u0}$ for two values of $M < 2N$ (see Figs. 2 and 3). Analysis of the obtained data allows us to draw a general conclusion: for films with the exchange energy larger than the energy of the random uniaxial magnetic anisotropy ($F^e/F^a > 1$) a satisfactory accuracy of the $\chi(f)$ calculation can be achieved for M of about 0.1% of the total number of modes $2N$. For films with $F^e/F^a < 1$ it is impossible in general to make such an estimate.

For the film model of size $N = 128 \times 128 \times 1$ noticeable ‘oscillations’ can be observed on $\chi(f)$ curve which are most pronounced for the films with ‘large’ crystallites. We assume that the source of this ‘oscillations’ is the insufficient averaging of integral magnetic characteristics of the film because of a small number of crystallites used in the model. The results of $\chi(f)$ calculations (plotted by dash line in Figs. 2 and 3) obtained with the use of Method 2 for $N = 1024 \times 1024 \times 1$ confirm this suggestion. It can be seen that the calculation of the magnetic susceptibility for the film models with a larger number of crystallites results in smoother curves.

4. Conclusion

In this paper, two numerical micromagnetic methods for calculation of the high frequency magnetic susceptibility of nanocrystalline thin films were considered in detail. An analysis of the methods enabled us to draw several conclusions about their advantages and shortcomings and specifics of their practical application.

The method based on series expansion of the solution of the system of linearized Landau–Lifshitz differential equations in terms of

eigenvectors of the normal magnetic oscillations modes has an important advantage. This method makes it possible to calculate not only the magnetic susceptibility of the nanocrystalline films but also to determine the structure of the spectrum of resonance modes excited by an external alternating magnetic field. In particular, this enabled us to reveal an additional excitation peak in the spectrum of nanocrystalline films which nature will be considered in our subsequent paper.

The main drawback of this method is its high requirements to memory capacity and calculation time. The computation of all eigenmodes in the general case of N computational cells required $O(4N^2)$ operations and bytes of RAM. The commonly used in practice approach for reducing the computational cost by decreasing the total number of eigenmodes used in calculation is applicable only to nanocrystalline films with the exchange energy larger than the energy of the random magnetic anisotropy.

On the other hand, the undetermined coefficients method for the solution of the system of linearized Landau–Lifshitz equations has a lower computational complexity. The computational time and memory of the method scale as $O(2N)$. Therefore, the undetermined coefficients method is more suitable to model high frequency characteristics of real thin nanocrystalline magnetic films.

Acknowledgments

This work was supported by the Ministry of Education and Science of the Russian Federation, № RFMEFI60417X0179.

References

- [1] J. Petzold, Advantages of softmagnetic nanocrystalline materials for modern electronic applications, *J. Magn. Magn Mater.* 242–245 (2002) 84, [https://doi.org/10.1016/S0304-8853\(01\)01206-9](https://doi.org/10.1016/S0304-8853(01)01206-9).
- [2] M. Yamaguchi, K.H. Kim, S. Ikeda, Soft magnetic materials application in the RF range, *J. Magn. Magn Mater.* 104 (2006) 208, <https://doi.org/10.1016/j.jmmm.2006.02.143>.
- [3] V. Dubuget, S. Dubourg, P. Thibaudeau, F. Duverger, Magnetic anisotropy dispersion with exchange energy in soft ferromagnetic thin films, *IEEE Trans. Magn.* 46 (2010) 1139, <https://doi.org/10.1109/TMAG.2010.2040187>.
- [4] B.A. Belyaev, A.V. Izotov, P.N. Solovov, Competing magnetic anisotropies in obliquely deposited thin permalloy film, *Physica B* 481 (2016) 86, <https://doi.org/10.1016/j.physb.2015.10.036>.
- [5] X. Ou, J. He, Z. Xia, J. Hao, Yu Wang, J. An, S. He, D. Zhao, Improvement of microwave permeability spectra in high stacking density FeNi nanoparticle films prepared by electric field-assisted deposition, *Appl. Phys. A* 123 (2017) 406, <https://doi.org/10.1007/s00339-017-1023-1>.
- [6] F. Xu, S. Li, C.K. Ong, Extrinsic damping contribution in soft magnetic thin films detected by permeability spectra, *J. Appl. Phys.* 109 (2011) 07D322, <https://doi.org/10.1063/1.3549611>.
- [7] A.N. Lagarkov, K.N. Rozanov, High-frequency behavior of magnetic composites, *J. Magn. Magn Mater.* 321 (2009) 2082, <https://doi.org/10.1016/j.jmmm.2008.08.099>.
- [8] W.F. Brown, *Micromagnetics*, Wiley, New York, 1963.
- [9] D. Kumar, A.O. Adeyeye, Techniques in micromagnetic simulation and analysis, *J. Phys. D Appl. Phys.* 50 (2017) 343001, <https://doi.org/10.1088/1361-6463/aa7c04>.
- [10] D.V. Berkov, N.L. Gorn, Numerical simulation of the magnetization structures in thin polycrystalline films with the random anisotropy and intergrain exchange, *J. Appl. Phys.* 83 (1998) 6350, <https://doi.org/10.1063/1.367913>.
- [11] B.A. Belyaev, A.V. Izotov, P.N. Solovov, Numerical simulation of magnetic microstructure in nanocrystalline thin films with the random anisotropy, *J. Siberian Federal Univ. - Math. Phys.* 10 (2017) 132, <https://doi.org/10.17516/1997-1397-2017-10-1-132-135>.
- [12] S.V. Komogortsev, V.A. Fel'k, R.S. Iskhakov, G.V. Shadrina, Micromagnetism in a planar system with a random magnetic anisotropy and two-dimensional magnetic correlations, *J. Exp. Theor. Phys.* 125 (2017) 323, <https://doi.org/10.1134/S1063776117070196>.
- [13] B.A. Belyaev, A.V. Izotov, An. A. Leksikov, Micromagnetic calculation of the equilibrium distribution of magnetic moments in thin films, *Phys. Solid State* 52 (2010) 1664, <https://doi.org/10.1134/S1063783410080160>.
- [14] P.N. Solovov, A.V. Izotov, B.A. Belyaev, Microstructural and magnetic properties of thin obliquely deposited films: a simulation approach, *J. Magn. Magn Mater.* 429 (2017) 45, <https://doi.org/10.1016/j.jmmm.2017.01.012>.
- [15] P.N. Solovov, A.V. Izotov, B.A. Belyaev, Micromagnetic simulation of magnetization reversal processes in thin obliquely deposited films, *J. Siberian Federal Univ. - Math. Phys.* 9 (2016) 524, <https://doi.org/10.17516/1997-1397-2016-9-4-524-527>.
- [16] R.D. McMichael, D.J. Twisselmann, A. Kunz, Localized ferromagnetic resonance in

- inhomogeneous thin films, *Phys. Rev. Lett.* 90 (2003) 227601, <https://doi.org/10.1103/PhysRevLett.90.227601>.
- [17] N.G. Chechenin, Ultra-soft magnetic films: micromagnetism and high frequency properties, *Microelectron. Eng.* 81 (2005) 303, <https://doi.org/10.1016/j.mee.2005.03.024>.
- [18] A.J. Newell, W. Williams, D.J. Dunlop, A generalization of the demagnetizing tensor for nonuniform magnetization, *J. Geophys. Res.* 98 (1993) 9551, <https://doi.org/10.1029/93JB00694>.
- [19] B. Van de Wiele, F. Olyslager, L. Dupre', D. De Zutter, On the accuracy of FFT based magnetostatic field evaluation schemes in micromagnetic hysteresis modeling, *J. Magn. Magn Mater.* 322 (2010) 469, <https://doi.org/10.1016/j.jmmm.2009.09.077>.
- [20] A.G. Gurevich, G.A. Melkov, *Magnetization Oscillations and Waves*, (1996) Boca Raton, Florida, United States.
- [21] M. Grimsditch, L. Giovannini, F. Monotcello, F. Nizzoli, G.K. Leaf, H.G. Kaper, Magnetic normal modes in ferromagnetic nanoparticles: a dynamical matrix approach, *Phys. Rev. B* 70 (2004) 054409, <https://doi.org/10.1103/PhysRevB.70.054409>.
- [22] K. Rivkin, J.B. Ketterson, Micromagnetic simulations of absorption spectra, *J. Magn. Magn Mater.* 306 (2006) 204, <https://doi.org/10.1016/j.jmmm.2006.02.245>.
- [23] M. d'Aquino, C. Serpico, G. Miano, C. Forestiere, A novel formulation for the numerical computation of magnetization modes in complex micromagnetic systems, *J. Comput. Phys.* 228 (2009) 6130, <https://doi.org/10.1016/j.jcp.2009.05.026>.
- [24] A.V. Izotov, B.A. Belyaev, A method for computing the microwave absorption spectrum in a discrete model of a ferromagnetic, *Russ. Phys. J.* 53 (2011) 900, <https://doi.org/10.1007/s11182-011-9508-4>.
- [25] B.A. Belyaev, A.V. Izotov, Micromagnetic calculation of magnetostatic oscillation modes of an orthogonally magnetized disk of yttrium iron garnet, *Phys. Solid State* 55 (2013) 2491, <https://doi.org/10.1134/S1063783413120068>.
- [26] S. Labbe, P.-Y. Bertin, Microwave polarizability of ferrite particles with non-uniform magnetization, *J. Magn. Magn Mater.* 206 (1999) 93, [https://doi.org/10.1016/S0304-8853\(99\)00537-5](https://doi.org/10.1016/S0304-8853(99)00537-5).
- [27] N. Vukadinovic, O. Vacus, M. Labrune, O. Acher, D. Pain, Magnetic excitations in a weak-stripe-domain structure: a 2D dynamic micromagnetic approach, *Phys. Rev. Lett.* 85 (2000) 2817, <https://doi.org/10.1103/PhysRevLett.85.2817>.
- [28] N. Vukadinovic, Dynamic micromagnetic simulations of susceptibility spectra in thin films with nonuniform magnetization distributions, *IEEE Trans. Magn.* 38 (2002) 2508, <https://doi.org/10.1109/TMAG.2002.801908>.
- [29] C. Vaast-Paci, L. Leylekian, Numerical simulations of isolated particles susceptibilities: effects of shape and size, *J. Magn. Magn Mater.* 237 (2001) 342, [https://doi.org/10.1016/S0304-8853\(00\)01362-7](https://doi.org/10.1016/S0304-8853(00)01362-7).
- [30] N. Vukadinovic, High-frequency response of nanostructured magnetic materials, *J. Magn. Magn Mater.* 321 (2009) 2074, <https://doi.org/10.1016/j.jmmm.2009.01.049>.
- [31] K.M. Lebecki, M.J. Donahue, M.W. Gutowski, Periodic boundary conditions for demagnetization interactions in micromagnetic simulations, *J. Phys. D Appl. Phys.* 41 (2008) 175005, <https://doi.org/10.1088/0022-3727/41/17/175005>.
- [32] G. Herzer, Nanocrystalline soft magnetic materials, *J. Magn. Magn Mater.* 157/158 (1996) 133, [https://doi.org/10.1016/0304-8853\(95\)01126-9](https://doi.org/10.1016/0304-8853(95)01126-9).